toxins

MDPI

Article

Production, Characterisation and Testing of an Ovine Antitoxin against Ricin; Efficacy, Potency and Mechanisms of Action

Sarah J. C. Whitfield, Gareth D. Griffiths, Dominic C. Jenner, Robert J. Gwyther, Fiona M. Stahl, Lucy J. Cork, Jane L. Holley, A. Christopher Green * and Graeme C. Clark *

Chemical, Biological and Radiological Division, Dstl, Porton Down, Salisbury SP4 0JQ, UK; SJWHITFIELD@dstl.gov.uk (S.J.C.W.); dcjenner@dstl.gov.uk (D.C.J.); RJGWYTHER@dstl.gov.uk (R.J.G.); fmstahl@dstl.gov.uk (F.M.S.); ljcork@dstl.gov.uk (L.J.C.); jlholley@dstl.gov.uk (J.L.H.)
* Correspondence: acgreen@dstl.gov.uk (A.C.G.); gcclark@dstl.gov.uk (G.C.C.)

Academic Editors: Julien Barbier and Daniel Gillet
Received: 4 September 2017; Accepted: 13 October 2017; Published: 18 October 2017

Abstract: Ricin is a type II ribosome-inactivating toxin that catalytically inactivates ribosomes ultimately leading to cell death. The toxicity of ricin along with the prevalence of castor beans (its natural source) has led to its increased notoriety and incidences of nefarious use. Despite these concerns, there are no licensed therapies available for treating ricin intoxication. Here, we describe the development of a F(ab')$_2$ polyclonal ovine antitoxin against ricin and demonstrate the efficacy of a single, post-exposure, administration in an in vivo murine model of intoxication against aerosolised ricin. We found that a single dose of antitoxin afforded a wide window of opportunity for effective treatment with 100% protection observed in mice challenged with aerosolised ricin when given 24 h after exposure to the toxin and 75% protection when given at 30 h. Treated mice had reduced weight loss and clinical signs of intoxication compared to the untreated control group. Finally, using imaging flow cytometry, it was found that both cellular uptake and intracellular trafficking of ricin toxin to the Golgi apparatus was reduced in the presence of the antitoxin suggesting both actions can contribute to the therapeutic mechanism of a polyclonal antitoxin. Collectively, the research highlights the significant potential of the ovine F(ab')$_2$ antitoxin as a treatment for ricin intoxication.

Keywords: ricin; antibody; antitoxin; efficacy; intracellular trafficking

1. Introduction

Ricin is a toxic protein obtained from the seeds of the castor oil plant (*Ricinus communis*) which is grown commercially in many parts of the developing world for castor oil production. Although approximately 1000-fold less toxic than the botulinum toxins, ricin is considered a potential biological warfare agent because of the ease and rapidity with which large quantities can be produced and the wide availability of castor beans [1,2]. Historically, it has been employed in many criminal activities and recently it has been considered a weapon of choice for extremist and terrorist groups [3]. A significant number of fatal and sub-lethal cases of human intoxication have been reported following accidental or deliberate ingestion or from parenteral exposure to ricin [4]. The development of prophylactic and post-exposure therapies for ricin intoxication has been on-going for many years [5,6] and a continued requirement for the development of medical countermeasures for ricin has been identified [7]. At present, however, there is no specific prophylactic or post-exposure therapy available for the clinical management of individuals exposed to ricin.

Ricin is a 66 kilodalton (KDa) glycoprotein cytotoxin consisting of two polypeptide chains, termed the A-chain and the B-chain, which are linked by an easily reduced disulphide bond [8–10]. The toxin

binds via its B chain to terminal galactose residues found on the surface of many cells and also via both the A and B chain to mannose receptors found on specific cell populations [11–13]. Following intra-nasal administration of ricin, the toxin binds initially to lung epithelia and subsequently to immune cells (e.g., macrophages and dendritic cells) [14]. This binding event triggers the endocytic uptake of the toxin into the cell. Once internalised the ricin is transported via the trans-Golgi network into the endoplasmic reticulum lumen where the enzymatically active A chain is translocated into the cytosol [15]. The toxin then enzymatically inactivates the ribosome though depurination of a single adenine residue in the 28 S ribosomal subunit. This event inactivates the 60 S ribosomal subunit, disrupts protein synthesis and results in cell death [1,6]. A single ricin molecule has been hypothesised to have the potential to inactivate multiple ribosomes and consequently killing a cell [16–18]. Ricin also causes wider pathological issues such as vascular leakage, pulmonary oedema (in part though uncontrolled cellular recruitment), cytokine storm and, ultimately, the death of the exposed individual though an acute respiratory distress syndrome (ARDS)-like condition [19–21]. Mitigating these wider impacts of acute lung injury caused by ricin intoxication is important; has led to testing of novel immunotherapeutic approaches; and has been linked to the efficacy of candidate therapies [22,23].

The various animal models available to study ricin intoxication were reviewed by Roy et al. [24]. The pathological effects and subsequent clinical signs of ricin intoxication depend on the route of exposure, as this dictates the subsequent tissue distribution of the toxin [25]. Following intravenous or intramuscular administration, lesions eventually develop in the spleen, liver and kidneys [26,27] whilst the lung remains unaffected [25]. After oral ingestion, the gastrointestinal tract is severely affected [28,29]. Inhalational exposure produces effects that are mainly confined to the respiratory tract [30,31]. Rhesus macaques exposed to a sub-lethal challenge with ricin exhibited dyspnea, tachypnea, laboured breathing and anorexia. These signs decreased substantially within 48–60 h and pathologically resulted in a sub-acute/chronic reparative process in the lung [31]. Retention of radio-labelled toxin within the lung has also been demonstrated using murine models of exposure perhaps explaining the extensive localised tissue damage caused by ricin [27]. However, despite often irreversible damage having been caused to cells there are often no visible signs of intoxication in animals exposed to low doses of ricin. The presence of a lag phase in the appearance of signs of intoxication is related to the dose of ricin and by the route by which the toxin was administered [25,28,29]. The delayed appearance of clinical signs and a narrow window for the post-exposure administration of antitoxin therapies, which are key aspects for an effective medical response to a ricin incident, means the diagnosis and subsequent treatment of ricin intoxication are technically challenging.

Neutralising antibodies, raised in animals, are often used for treatment of intoxication and are effective if passive immunisation occurs prophylactically or shortly after exposure to the toxin [1,32,33]. Prophylactic administration of IgG or antibody-fragments (e.g., $F(ab')_2$ and Fab'), which often have an improved bioavailability compared to the whole IgG molecule, can provide protection against subsequent toxin exposure [32–35]. In addition, antibody-fragments typically have a reduced incidence of adverse anaphylactoid or anaphylactic reactions on single or repeat administration of antitoxin than do IgG-based antitoxins [33,36,37].

The window of opportunity (WOO) for administration of therapeutic antibodies against ricin has been shown to be between 0 and ~8 h for full protection [38–40] and longer, 18–72 h for partial protection [41,42]. Here, we have evaluated a purified, despeciated, $(Fab')_2$ polyclonal ovine antibody made to Good Manufacturing Practice (GMP) which has also demonstrated a long window of opportunity for an antibody-based therapeutic; offering full protection up to 24 h and partial protection when administered up to 30 h after an inhaled aerosol ricin challenge. This route of intoxication is considered to be a key route of exposure for which treatment is required in a biodefense context [1,3,5]. In the process of conducting these studies, we have also established in vitro and in vivo neutralization assays to assess the potency of the antitoxin for the determination of the consistency of the manufacturing process and for batch release and stability studies. In parallel, we used cutting

edge imaging flow cytometry methods to provide new insights in to the effects of this antitoxin on the uptake and intracellular transport of ricin that may contribute to its protective actions.

2. Results

2.1. Determination of the Ricin Neutralising Activity of the Antitoxin In Vitro

Prevention of the in vitro cytotoxic effects of ricin was used as a measure of the neutralizing activity of the antitoxin. Ricin at increasing concentrations and in the absence of the antitoxin produced a concentration-dependent cell death over 48 h in Vero cell cultures as measured by the WST-1 cell viability assay (Figure 1A). The LC_{50} (the concentration of ricin which kills 50% of the cell population) was determined to be 0.051 ng·mL^{-1}, with a 95% confidence interval (CI) of 0.030 to 0.089 ng·mL^{-1} (Figure 1A). Although the cell viability data were routinely normalized to control (100%) values, inconsistencies across the culture plates meant that on occasions more accurate and reliable estimates of the IC_{50} of ricin and EC_{50} of antitoxin were obtained using the top plateau of the viability data to define the maximum viability in an experiment (Figure 1A). It was also noted that in these assays ricin did not appear to result in complete loss of cell viability with a small ~10–20% WST 1 signal persisting at high ricin concentrations (Figure 1A,B) either because of a minor proportion of resistant cells or residual active dehydrogenase retained in cellular fragments. Premixing the ricin with antitoxin prior to addition of the mixture to the cells resulted in a very steep concentration-dependent protection of the cells from the cytotoxic effects of ricin (Figure 1B). The EC_{50} in this case was 377 ng·mL^{-1} (95% CI of 337 to 422 ng·mL^{-1}). Assuming that at the EC_{50} concentration the amount of free ricin must be equal to that causing 50% cell death, i.e., equivalent to the ricin LC_{50}, a neutralising ratio (µg of antitoxin required to neutralize 1 µg of ricin) can be calculated using Equation (1). On this occasion, the neutralising ratio was 106:1. Although characterisation using an ELISA approach suggests approximately 40% of the antitoxin is anti-ricin $F(ab')_2$, the neutralising ratios presented have not been corrected and are based upon the total protein content of the antitoxin material.

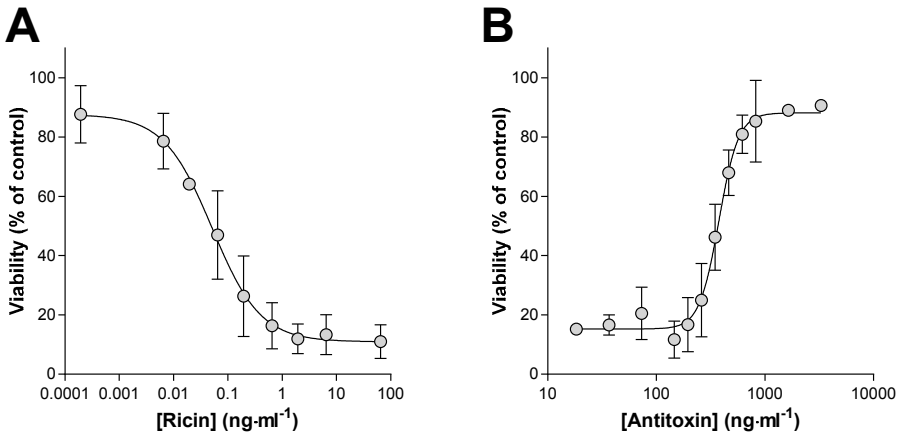

Figure 1. In vitro cytotoxicity of ricin and its neutralization by antitoxin. (**A**) Ricin caused a concentration dependent cytotoxicity in Vero cell cultures. (**B**) Pre-incubation of ricin (3.24 ng·mL^{-1}) with the indicated concentration of antitoxin resulted in neutralization of the cytotoxic effects of ricin. LC_{50} and EC_{50} values were determined from the 4-parameter logistical curve fits shown and used to calculate the neutralizing ratio as described in the main text. Data are shown as mean ± SD from three independent experiments in each case.

This cytotoxicity assay was characterized and validated sufficiently to support the production of antitoxin to Good Manufacturing Practice (GMP) standards and it enabled the evaluation of the ricin antitoxin potency and its stability during production and storage. The stability of the antitoxin, when stored at 2–8 °C, was tested using this assay at regular intervals from 0 to 72 months. Overall, there

was no decrease in potency over this time period (data not shown), and the mean neutralising ratio, calculated from all 24 determinations, was 108:1.

2.2. Determination of the Ricin Neutralising Activity of the Antitoxin In Vivo

The ricin neutralising activity of the antitoxin was also determined in vivo by measuring the protection afforded in mice following intraperitoneal (i.p.) administration of ricin alone and of ricin premixed with increasing amounts of antitoxin. Increasing doses of ricin resulted in earlier deaths (Figure 2A) and a progressive increase in the probability of death (Figure 2A,B). Analysis of the dose–lethality data using a probit response model gave an LD_{50} for i.p. ricin of 0.377 μg·mouse^{-1} (95% CI 0.358–0.397 μg·mouse^{-1}). The LD_{99} dose of ricin was estimated to be 0.61 μg·mouse^{-1} (95% CI 0.549–0.705 μg·mouse^{-1}). Doses of ricin in excess of this would be expected to kill all animals challenged and therefore the administration of a challenge dose of 2 μg (approximately $6LD_{50}$) was selected for use during the neutralisation study. The majority of mice challenged with this dose of ricin died within two days with weight loss and signs of intoxication being apparent after only 24 h (Figure 3C,D).

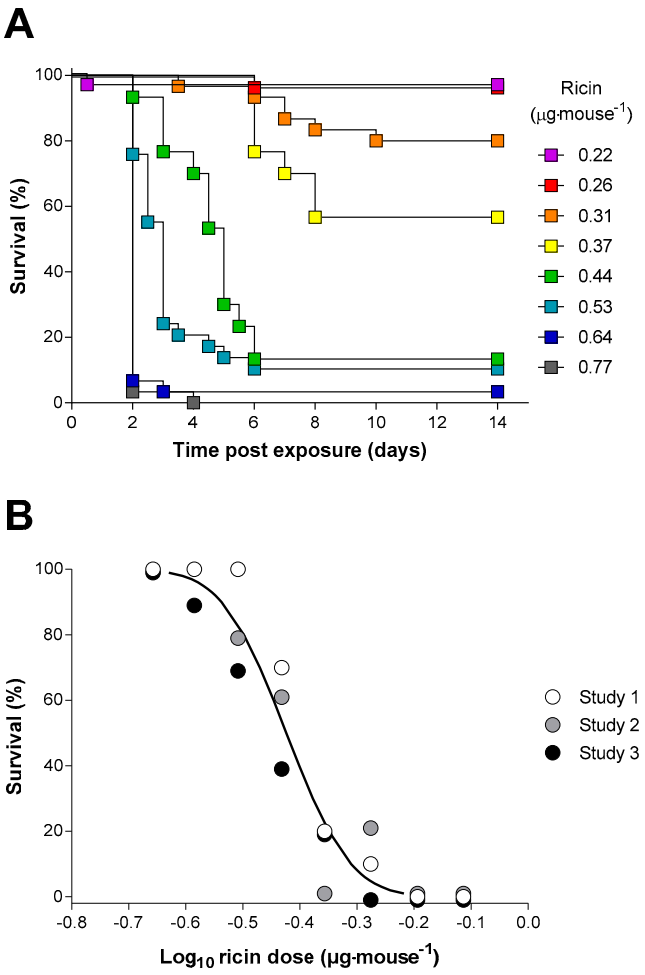

Figure 2. Ricin toxicity via the intraperitoneal (i.p.) route in the Balb/C mouse. (**A**) Kaplan–Meier plot of mouse survival following administration of the indicated concentrations of ricin. Data are shown for the combined studies, n = 30 for each dose. (**B**) Probit analysis of percentage survival of mice against the dose of ricin received: the curve was reconstructed from the output of the Minitab probit analysis, which was fitted to the combined dataset. Data points are shown as survival at 14 days from three independent experiments each with 10 mice per dose.

Increasing amounts of antitoxin, premixed with the ricin prior to i.p. administration, resulted in a delayed time to death and a protection from lethality which was dependent on the dose of antitoxin administered with the ricin challenge (Figure 3A,B). There was also a dose dependent decrease in the rate, and absolute amount, of weight loss (Figure 3C), and in a reduced score for clinical signs of intoxication (Figure 3D). For all but the highest doses of antitoxin, surviving animals exhibited signs of intoxication which persisted for 14 days after challenge at which point the experiment was terminated. In these studies, a small number of animals survived at low antitoxin doses probably because of misplaced i.p. injections [43]. Data from these animals was however included in the probit analysis which determined an ED_{50} for the antitoxin of 80 μg·mouse^{-1} (95% CI 79–81 μg·mouse^{-1}) and probit slope of 33 demonstrating a very steep dose–response relationship. The neutralising ratio (NR) can again be calculated based on the principles previously described (Section 2.1) and using Equation (2). Using this in vivo method, the neutralising ratio was determined to be 49:1.

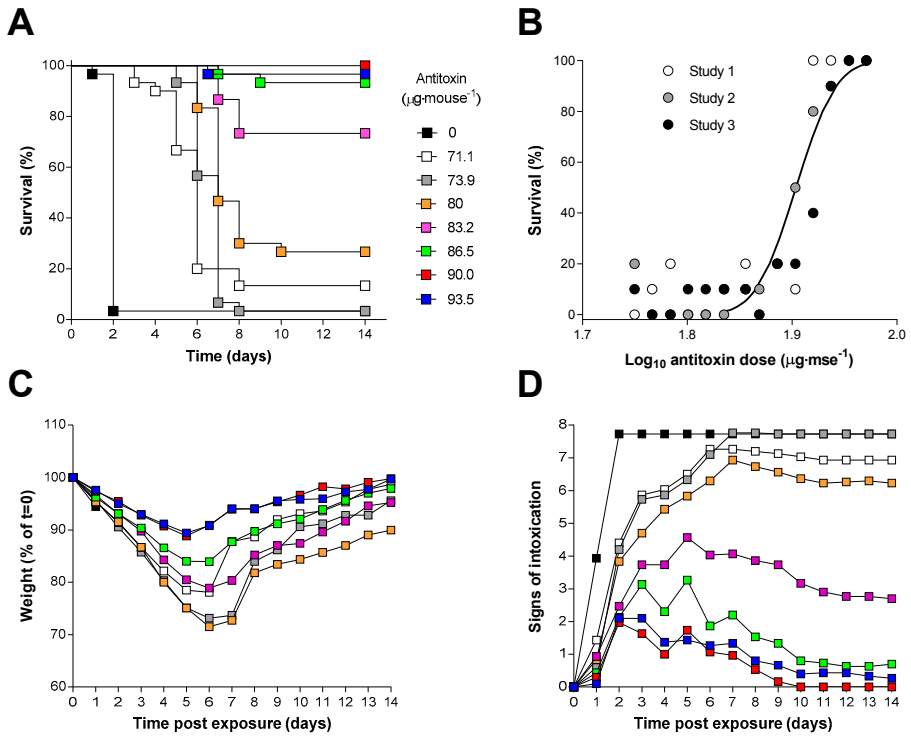

Figure 3. An in vivo neutralising assay in Balb/C mice. (**A**) Kaplan–Meier plot of survival in mice administered ricin (2 μg) pre-incubated with the indicated dose of antitoxin (the key shown in (**A**) also applies to (**C**,**D**)). Data are combined for three independent experiments (n = 30). (**B**) Probit analysis of survival at 14 days: the curve was reconstructed from the output of the Minitab probit analysis which was fitted to the combined dataset. Data points are shown for survival at 14 days from three independent experiments. (**C**,**D**) Body weight and signs of intoxication following administration of ricin and the indicated amount of antitoxin are shown. Data are combined from three independent experiments. Error bars have been omitted for clarity; the SDs are generally <10% and <2 units, respectively, for n = 30 mice in each dose group at the start of the study. Body weights are reported for all surviving animals at a particular time point. Signs of intoxication were scored according to Table S1.

2.3. Inhalation Toxicity of Ricin in Balb/C Mice

The efficacy of the antitoxin against an inhalation challenge to aerosolised ricin was determined in mice. Exposure of mice, head only, to increasing doses of ricin resulted in shorter times to death and increased probability of death (Figure 4A,B). Analysis of this dose–lethality data using a logistic model gave an estimate for the LCt_{50} of 7.2 mg·min·m^{-3} (95% CI 6.2–8.3 mg·min·m^{-3}).

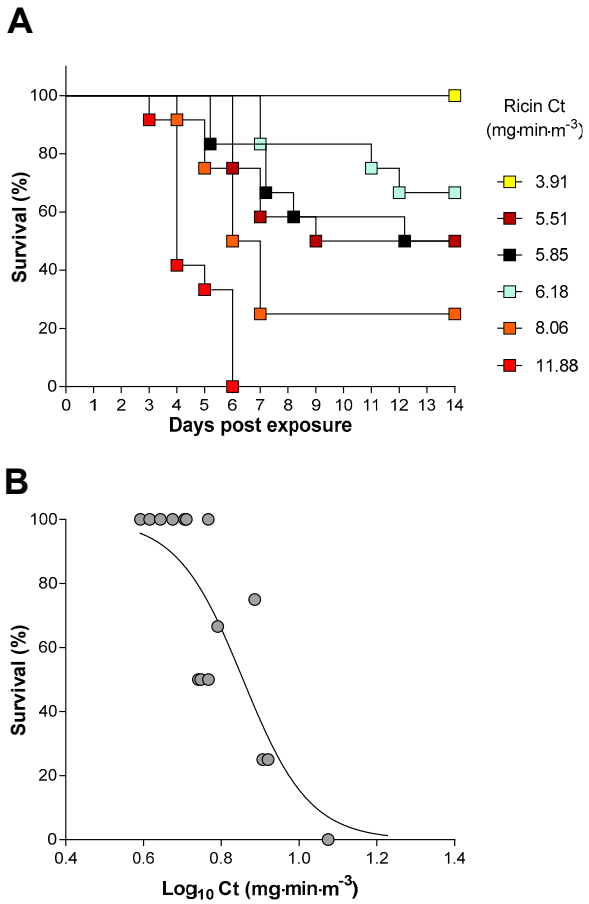

Figure 4. Characterisation of an inhalation model of ricin intoxication in Balb/C mice. (**A**) Kaplan–Meier plot of survival in groups of 12 mice following the head only exposure to the indicated Ct of ricin aerosol. (**B**) Dose–response analysis of survival at 14 days following inhalation of the indicated Ct of ricin aerosol. Each data point is from a group of 12 mice.

A similar analysis using data corrected for total ventilatory volume during exposure, obtained from plethysmography, gave an LD_{50} for the total inhaled dose of 10.4 $\mu g \cdot kg^{-1}$ (95% CI 9.3–11.6 $\mu g \cdot kg^{-1}$) (data not shown).

The estimated LCt_{99}, 17.7 $mg \cdot min \cdot m^{-3}$ (95% CI 9.0–24.8 $mg \cdot min \cdot m^{-3}$) was less than the challenge dose selected for the efficacy studies, $3LCt_{50}$, 21.5 $mg \cdot min \cdot m^{-3}$, and thus all animals exposed to this challenge dose were expected to die as a result of the ricin exposure. Indeed, all animals exposed to $3LCt_{50}$ of ricin succumbed to its lethal effects within 3–5 days of exposure (Figures 5A and 6A) and during this time they lost weight and exhibited typical signs of intoxication which were apparent in some mice by 24 h after exposure (Figure 5B,C).

2.4. Antitoxin Protection against an Inhalational Ricin Challenge

The efficacy of the antitoxin against an inhalation challenge to $3LCt_{50}$ of aerosolised ricin was assessed in mice. Antitoxin was administered via the intravenous route (i.v.) at 16, 24 or 30 h after the ricin challenge to determine the window of opportunity for effective antitoxin therapy. Survival was seen in all mice given a single 2.5 mg dose of antitoxin at the 16 and 24 h time points after ricin exposure. This antitoxin dose was selected because it was found to be an effective dose in preliminary and limited dose–response experiments (data not shown). A "breakthrough" in protection was observed when the ricin antitoxin was given 30 h after the ricin aerosol challenge, where 75% protection was achieved (Figure 5A). Greater weight loss was seen in mice where ricin antitoxin was

given at later time points (Figure 5B) suggesting that the quality of protection in surviving animals also decreased as antitoxin administration was delayed. Antitoxin administration had little effect on the observed signs of intoxication up to 48 h after ricin challenge however, whereas the control mice continued to develop more severe signs of intoxication, those treated with antitoxin gradually recovered over the next 12 days (Figure 5C). Control mice exposed to aerosolized vehicle only and given ricin antitoxin via the i.v. route after 16 h showed no weight loss or observed signs of intoxication (Figure 5B,C).

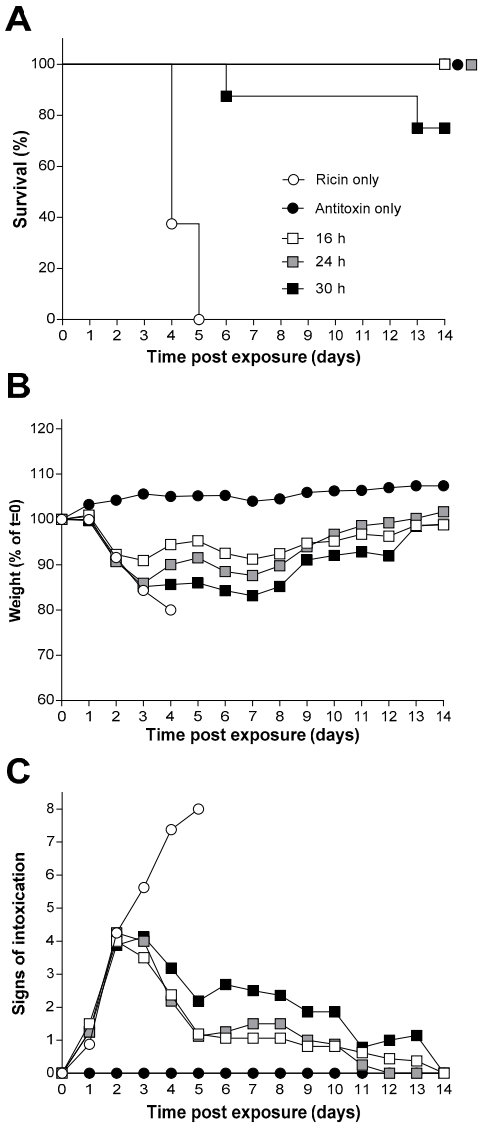

Figure 5. The window of opportunity for effective ricin antitoxin therapy following inhalational exposure of Balb/C mice to ricin. (**A**) Kaplan–Meier plot of survival in treated with antitoxin (2.5 mg·mouse^{-1}) at the indicated times after challenge with 3LCt$_{50}$ of ricin (the key shown in (**A**) also applies to (**B**,**C**). Data are from groups of eight mice in each case. (**B**,**C**) Body weight and signs of intoxication following administration of ricin and the indicated amount of antitoxin are shown. Data are combined from three independent experiments. Error bars have been omitted for clarity; the SDs are generally <10% and <2 units, respectively, for n = 8 mice in each group. Signs of intoxication were scored according to Table S1.

For assessment of the dose-dependence of the antitoxin-mediated protection, antitoxin or vehicle was administered to mice that had been exposed to ricin by the inhalational route 20 h earlier. This

time point was chosen, as it was logistically more convenient for the experimental design than a 24 h administration time. Control animals challenged with ricin and administered antitoxin vehicle died or reached the humane endpoint within five days of exposure as expected (Figure 6A). Antitoxin administration produced a dose-dependent increase in the time to death (Figure 6A) and a dose dependent increase in survival at 14 days after challenge (Figure 6A,B). Antitoxin-mediated protection had an ED_{50} of 162 μg·mouse^{-1} (95% CI 133 to 196 μg·mouse^{-1}) by probit analysis.

Consistent with the affects observed within the intraperitoneal model, it was found that there was a dose-dependent decrease in both visible signs and weight loss associated increasing antitoxin dose administered (Figure 6C,D). Early signs of intoxication could be observed within a small number of animals after 24 h following challenge. However, between 24 h and 48 h, there is a rapid increase in the signs observed within the experimental animals representing a localised toxin-associated tissue damage triggering wider systemic issues (Figure 6D).

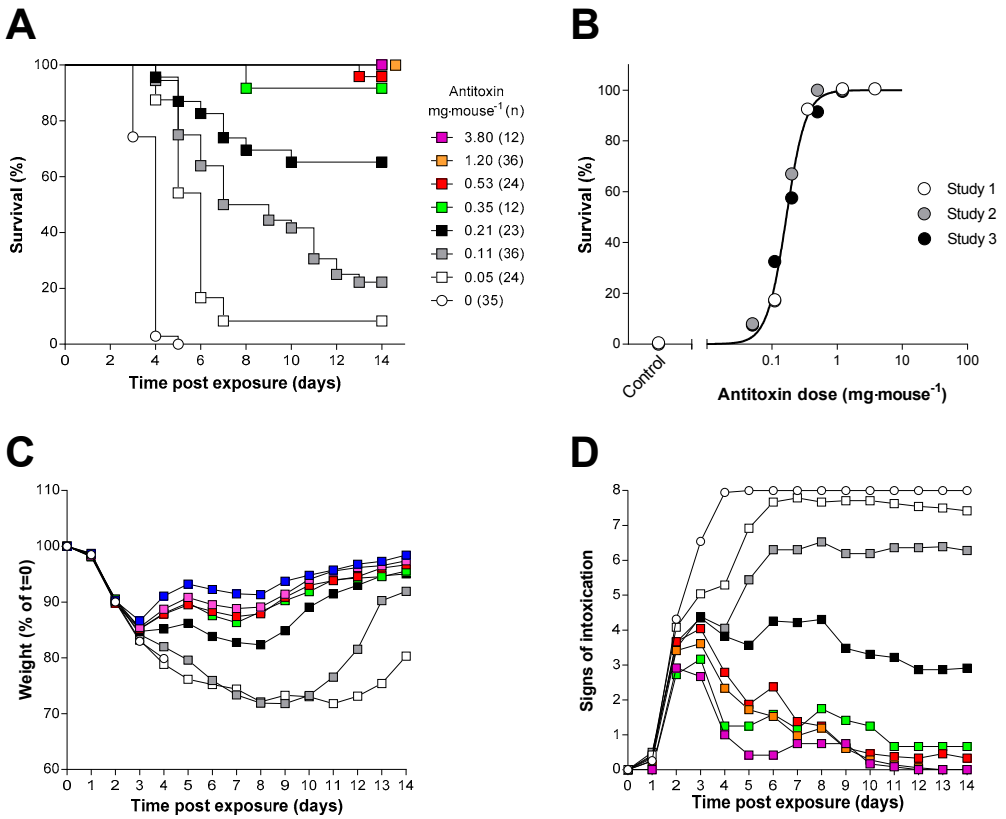

Figure 6. Characterisation of the dose–response of ovine F(ab')$_2$ in the mouse ricin inhalation model. (**A**) Kaplan–Meier plot of survival in mice administered ricin (3LCt_{50}, 21.54 mg·min·m^{-3}) and treated 20 h later with the indicated dose of antitoxin i.v. (the key in (**A**) also applies to (**C**,**D**)). Data have been combined from three independent experiments each of which used a group size of 12 mice. (**B**) Probit analysis of survival at 14 days, the curve was reconstructed from the output of the Minitab probit analysis which was fitted to the combined dataset. Data points are shown for survival at 14 days from three independent experiments. (**C**) Body weight; and (**D**) signs of intoxication following administration of ricin and the indicated amount of antitoxin are shown. Data are combined from three independent experiments. Error bars have been omitted for clarity; the SDs are generally <10% and <2 units, respectively, for n = 12–36 mice. Signs of intoxication were scored according to Table S1.

2.5. Antitoxin Can Affect the Uptake and Intracellular Trafficking of Ricin in A549 Cells

Cellular uptake and intracellular trafficking of the toxin in the presence or absence of antitoxin was examined to determine the mechanism of action of the antitoxin. A549 human lung epithelial cells

were used and labelled ricin was tracked using Imaging Flow Cytometry (IFC), allowing transport of the toxin to both the cytoplasm and the Golgi apparatus to be observed in the presence and absence of antitoxin. For this, ricin was either added alone or was pre-incubated with antitoxin (1 h at 37 °C) at two different ratios (1:20 and 1:50) prior to exposure of the cells for 15, 30 or 60 min (Figure 7A,B). Ricin was rapidly taken up by the cells appearing within the cytoplasmic mask of approximately 90% of the cells by 60 min (Figure 7A). Ricin antitoxin caused a concentration dependent reduction in the percentage of cells taking up ricin with the 1:50 ratio of ricin to antitoxin showing a 50% reduction in ricin positive cells at 60 min (Figure 7A).

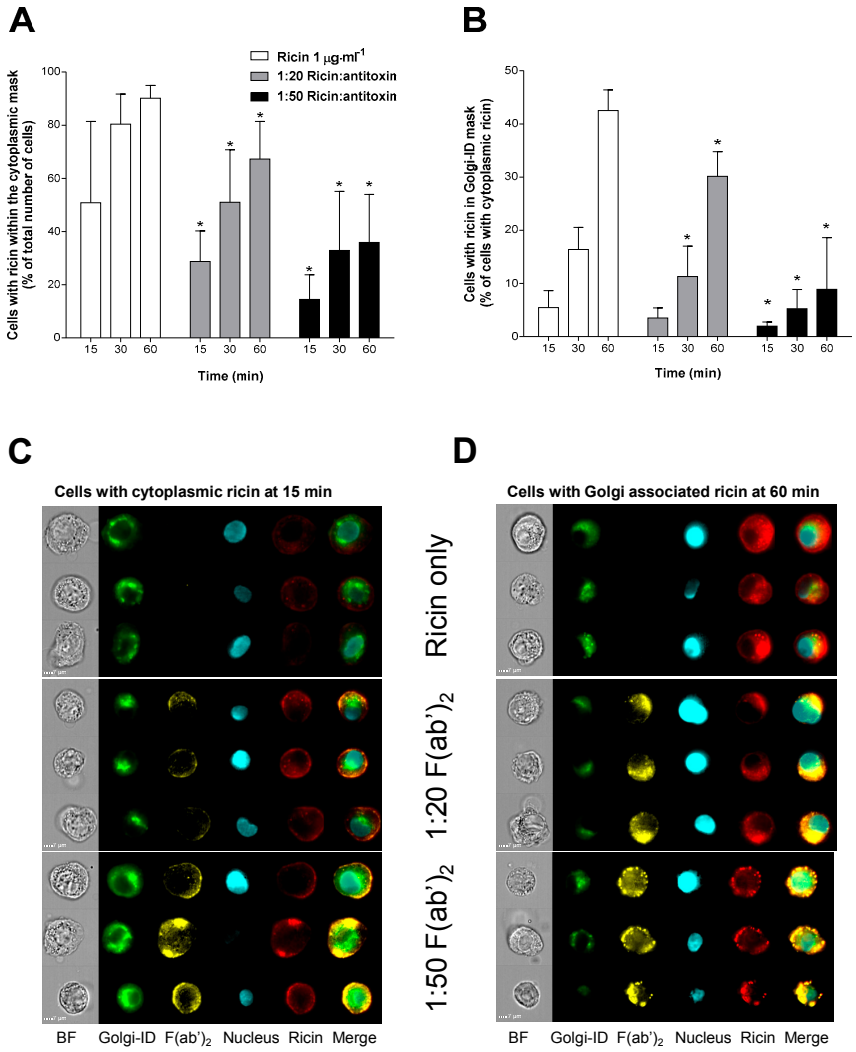

Figure 7. Effect of antitoxin on uptake and trafficking of ricin in human cultured A549 cells. (**A**) Antitoxin reduces cellular uptake and appearance of ricin within the cellular cytoplasmic mask in a concentration dependent manner. (**B**) In those cells that are positive for cytoplasmic ricin, antitoxin reduces the percentage of cells that have Golgi-associated ricin compared to control. Data in (**A**,**B**) are shown as mean ± SD from three independent experiments. * $p < 0.05$ (two-way ANOVA with multiple comparisons). (**C**,**D**) Example images of $F(ab')_2$ and ricin interactions at 15 and 60 min as shown as part of the ImageStreamX analysis (BF = Brightfield).

In the subset of cells that were ricin positive, the toxin became associated with the Golgi apparatus slowly over the time course of the study with only 40% of the cells with cytoplasmic ricin having the toxin also co-localising to the Golgi apparatus by 60 min (Figure 7B). Administration of the

ricin-antitoxin mixture markedly reduced the co-localisation of ricin and the Golgi apparatus in the cytoplasmic ricin positive cells, with statistically significant reductions at 30 and 60 min for the 1:20 ratio and at all time points for the 1:50 ratio (Figure 7B, $p < 0.05$ 2-way ANOVA) suggesting that the antitoxin affects intracellular trafficking of ricin to the Golgi apparatus. It can be seen from the flow cytometry images that the A549 cells accumulate both the ricin and antitoxin over the time course of the experiment and that these remain co-localised within the cell (Figure 7C,D).

3. Discussion

We have produced an antitoxin for treatment of ricin intoxication which is based on a ovine polyclonal anti-ricin IgG, despeciated to its $F(ab')_2$ fragments. The antitoxin was characterised in vitro and in vivo to determine its ability to neutralise ricin toxin and was shown to be effective in protecting mice against an inhalational challenge with aerosolised ricin. Importantly, the antitoxin demonstrated effective protection against the lethal effects of ricin when it was administered up to 30 h after the ricin challenge. Full protection was seen at 24 h and partial, 75%, protection was seen at 30 h. Efficacy at such delayed time points is likely to be necessary for effective treatment of ricin intoxication given that there is a delay in the appearance of signs of intoxication making confirmation of exposure, diagnosis of intoxication and the subsequent medical response, technically and logistically challenging. This is especially true considering that the potential use of ricin in military or civilian scenarios is unlikely to be predicted [1–3]. These data are therefore encouraging in that such long WOO may enable an effective medical response to a ricin incident, provided that this WOO is reproduced in other animal species and is predicted in man.

Whilst our data provide robust evidence that there is a post-exposure WOO for treatment of ricin intoxication, other authors have also described effective post-exposure treatment of ricin intoxication with anti-ricin antibodies. Many of these reports have highlighted the limited WOO for protection against the toxin, typically found to be up to ~8 h after ricin exposure [22,38–40]. There have however been reports of WOO similar to that described here however our research if the first to demonstrate full protection at 24 h. For example, Pratt et al. [41] used an oropharyngeal aspiration model to challenge mice with ricin. They were able to protect all of the ricin-exposed mice with polyclonal anti-ricin antibodies raised against deglycosylated ricin A chain when the antibodies were administered 18 h after challenge. When administered at 24 h after challenge this antibody preparation protected only 30% of the mice. RAC 18 is a monoclonal antibody also raised against ricin A chain. This antibody protected ~60% of ricin-challenged mice when administered at 18 h and ~50% when given after 24 h from intoxication [41]. Chimeric high affinity IgG antibodies originally isolated from rhesus macaques immunised with ricin holotoxin or subunit vaccine [44] have also been shown to provide an extended window of opportunity in an intranasal mouse model of ricin intoxication [42]. When administered 24 h after a $2LD_{50}$ ricin challenge, administration of the individual antibodies gave survival rates of between 62–89%. Furthermore, a cocktail of three antibodies, one directed at ricin A chain and two directed at the B chain resulted 80% survival at 24 h and statistically significant protections, 73% and 36%, when administered at 48 h or 72 h respectively [42]. It should be noted that direct comparison of the window of opportunity for treatment with antibody-based therapeutics is complicated by the different challenge and treatment doses and routes of exposure used. The lower challenge dose of ricin (i.e., $2LD_{50}$ via the intranasal route) used in an number of studies may represent a less stringent challenge model for assessing antitoxin treatment and may explain the longer times to death of ~4–9 days [42,44] when compared to the $3LCt_{50}$ inhalation challenge used in our experiments which results in death or humane end-point at 3–5 days post exposure. For our polyclonal antitoxin doses of 2.5 mg·mouse^{-1} (approximately 125 mg·kg^{-1}) were used to provide protection at 24 and 30 h and doses in excess of 0.8 mg·mouse^{-1} (approximately 40 mg·kg^{-1}) are predicted to provide full protection when administered at 20 h after intoxication (Figure 6). These doses are in excess of those typically required of monoclonal neutralising antibodies which, in the examples above, range from ~3 to ~17 mg·kg^{-1}. There is however little information available to inform how the

dose of antitoxin required for protection is related to the WOO making direct comparisons difficult. Irrespective of the differences in ricin challenge, our results and those detailed above demonstrate that following a pulmonary challenge with ricin, either directly with aerosolised ricin in the case of the data reported here or via intranasal instillation, there is a relatively long window of opportunity for effective treatment in mice that extends for 24 h or longer. Given that the antitoxin must physically interact with the ricin to bring about neutralisation of toxicity, these observations imply that toxicologically relevant amounts of ricin are accessible to antitoxin at these time points after exposure. This is perhaps unexpected as ricin is known to bind and be taken up rapidly by cells in culture [45]. This suggests that either the kinetics of ricin cellular uptake and trafficking, observed in vitro, are not reflected in vivo or that that the assumption of a purely extracellular mode of neutralisation is an incomplete explanation of the therapeutic mechanism of these antitoxins.

To examine these possibilities, in vitro studies to track labelled ricin and antitoxin were conducted in A549 pulmonary epithelial cells. As expected, ricin alone rapidly associated with and became internalised in the cells. The polyclonal antibody, when pre-incubated with ricin, reduced toxin uptake, demonstrating that interference with this process could contribute to protection. Ricin cellular binding and uptake is mediated by the ricin B chain, and this has typically been targeted by neutralising antibody strategies. B chain binders have previously been shown to be responsible for ricin vaccine efficacy [46] and to neutralise ricin in vitro and provide protection in vivo [47,48] with some B chain binders being superior to A chain binders in these assays [49]. Nevertheless, the A chain binders have been shown to be effective treatments for ricin intoxication [41,42,44] and thus can clearly contribute to protection.

The antitoxin used in our studies was raised in sheep against a formaldehyde toxoid of ricin holotoxin and will contain a polyclonal mix of both A and B chain binders. Interestingly it has been observed that both A and B chain directed anti-ricin antibodies have the ability to neutralise ricin activity intracellularly and can disrupt the intracellular trafficking of ricin [50–53]. Our data, from imaging flow cytometry studies, suggest that such effects can also be mediated by polyclonal antibody-fragment antitoxins and that such block or miss-direct of normal intracellular trafficking of ricin towards proteolytic or other non-toxic routes could contribute to the long therapeutic window for this antitoxin.

Anaphylactoid reactions, anaphylaxis and serum sickness are recognised complications that can result from passive immunisation with foreign antibody products [33,37], particularly if a large dose is needed to provide protection, as is likely to be the case with our antitoxin. Thus, a further difference between our antitoxin and monoclonal chimeric/humanised antibody approaches used by others [42,44,48] is that despeciation to create $F(ab')_2$ was considered necessary to reduce the likelihood of adverse immune reactions in any recipient [35,54]. In addition, an ovine source of hyperimmune plasma was selected as ovine antibodies are considered to be less immunogenic than those of equine or caprine origin [55,56]. Importantly, the protective efficacy of the $F(ab')_2$ antitoxin was found to be comparable with the parent IgG molecule [57] demonstrating that the Fc-mediated properties of the whole IgG molecule did not appear to be important in the overall protective mechanism. In the studies reported here, no immunotoxicological indices were monitored in the mice administered the 2.5 mg dose of antitoxin alone, however, these animals did show a normal body weight profile and no observed signs of intoxication (many of which are general indicators of health and wellbeing) over a subsequent 14 day observation period (Figure 5). It should be noted that our polyclonal antitoxin is currently in advanced development as a treatment for inhalational ricin intoxication. Whilst it has been manufactured to GMP and has shown efficacy, assessment of the safety, in animals, of the predicted protective dose is planned but has yet been undertaken and this will represent a regulatory challenge for the clinical development of the antitoxin. However, as there are no available treatments for ricin intoxication, the polyclonal antitoxin approach could still represent an effective and pragmatic approach for treatment of ricin inhalation, although consideration would need to be given to the management of side effects should they occur.

One of the key aims of this research was to reduce the numbers of animals required during the development of the antitoxin which requires potency determinations assessment of their stability at multiple time points and storage temperatures. For antitoxins, this has traditionally involved in vivo methodologies. However, Sesardic et al. [58] examined the antibodies raised against diphtheria toxoid in an in vitro Vero cell assay and compared potency within the guinea pigs concluding that there was a strong correlation between the potencies in both models. These models are now the basis of an international standard for characterising batches of human diphtheria antitoxin [59].

Here, work was undertaken to investigate the utility of an in vitro model using Vero cells for assessing potency and stability of the ricin antitoxin. The in vitro approach was used routinely and reproducibly in GMP processes to produce the antitoxin. Importantly, it demonstrated that the $F(ab')_2$ antitoxin product maintained its neutralising activity for at least 72 months after manufacture, a finding which was consistent with the physico-chemical properties of the antitoxin which were also unchanged over this period (data not shown). Comparison of the in vitro and in vivo neutralising assay has been conducted for the $F(ab')_2$ antitoxin with the ratio (antitoxin:ricin) being ~2 fold lower in vivo than in vitro. That the values are not identical may be due to the different factors involved in ricin toxicity in vitro and in vivo. For example, in vivo, clearance and binding to non-critical sites (sites that do not result in cytotoxicity or that do not link directly to lethality) may also contribute to protection and therefore less antitoxin might be needed to neutralise the remaining toxin. Whereas in vitro there is no clearance and all cytotoxicity counts towards the final assay result. Further studies with other antitoxins will be required to determine if this observation is a consistent feature of the in vitro and in vivo neutralising assay methods.

Antitoxins and other approaches to treatment of ricin intoxication such as small molecule retrograde transport inhibitors [60–62] or combinations of therapies such as antibiotics and antitoxins [63] could increase the WOO for effective treatment. Efficacy data in the mouse have been demonstrated for these approaches and, additionally, the research has also provided important mechanistic insights with regard to the properties of an effective therapy. However, as will be necessary for the antibody-based antitoxin developed here, further safety and efficacy studies will be required in other (higher) animal species for these approaches to gain approval for use in humans. Our current data add significantly to the current research field and provide evidence that a practicable mitigation for exposure to this potentially lethal, potent and readily-available ricin toxin should be achieved in the near future.

4. Conclusions

Passive immunity is a highly effective strategy for treating intoxications caused by ribosome inactivating proteins such as the ricin toxin. The development of antibody-based antitoxins that are effective when used many hours after exposure to the toxin will represent a step forward in the treatment of ricin-associated intoxication. We have produced an ovine polyclonal $F(ab')_2$ that can fully protect mice from the lethal effects of a $3LCt_{50}$ inhaled aerosol challenge with ricin at prolonged times that are comparable to those achieved with other polyclonal and/or monoclonal antitoxins. Full protection was observed at 24 h following challenge and partial protection at 30 h demonstrating that this polyclonal antitoxin has a wide window of opportunity commensurate with that required to represent a practicable approach to mitigate the effects of ricin intoxication.

5. Materials and Methods

5.1. Preparation of Ricin and Ricin Toxoid

Ricin toxin was prepared from the seeds of *Ricinus communis subspecies zanzibariensis* as previously described [64]. Ricin toxoid was produced by adding formaldehyde (Sigma Aldrich, Poole, UK) to a final concentration of 2.5% (w/v), (pH 7.10–7.30) and incubating at 37 °C for 14 days. Excess formaldehyde was quenched by the addition of lysine hydrochloride (Sigma Aldrich, Poole, UK) to a

final concentration of 0.1 M. The quenched material was then desalted into phosphate buffered saline (PBS) (Gibco, ThermoFisher Scientific, Loughborough, UK) using a 5.0 × 50 cm G25M Sephadex column. The protein concentration determined by BCA protein assay (ThermoFisher Scientific, Loughborough, UK), and formaldehyde added back to final concentration of 0.025% (w/v).

5.2. Preparation of Ovine Ricin Antitoxin and Despeciated Antitoxin Fragment F(ab')$_2$

Briefly, a polyclonal antibody (IgG) was produced from hyper-immune plasma that was raised in sheep (Selborne Biological Services, Tasmania, Australia) following immunisation with ricin toxoid at 6 weekly intervals. Sheep received a priming dose of ricin toxoid in Freund's Complete Adjuvant (Sigma Aldrich, Poole, UK) followed by booster doses of ricin toxoid in Freund's Incomplete Adjuvant at 6 weekly intervals (100 μg ricin toxoid per dose).

The production of F(ab')$_2$ was undertaken by International Therapeutic Proteins (ITP Ltd, Tasmania, Australia). In brief, IgG was purified from selected production bleeds that were taken between Week 14 and Week 38 of the immunisation schedule. The IgG was digested with pepsin (Sigma Aldrich, Poole, UK) to produce F(ab')$_2$ which was lyophilized to form a stable pellet and was stored at 2–8 °C. Prior to use the antitoxin was reconstituted with distilled water (Gibco, ThermoFisher Scientific, Loughborough, UK) and aliquots stored at −20 °C.

5.3. In Vitro Cytotoxicity Assay

Vero cells (ECACC 84113001) were obtained from the European Collection of Animal Cell Cultures (ECACC) (Public Health England, Salisbury, UK). Cells were maintained in culture medium consisting of DMEM (Sigma Aldrich, Poole, UK) with 10% (v/v) foetal calf serum (Sigma Aldrich, Poole, UK), 1% penicillin/streptomycin solution (containing 100 units·mL^{-1} penicillin and 0.01 mg·mL^{-1} streptomycin), and 1% (w/v) L-glutamine (Sigma Aldrich, Poole, UK) 2 mM. Vero cells were grown in 150 cm^2 flasks in a humidified atmosphere of 5% CO_2 in air at 37 °C and removed from the flask surface using incubation with trypsin (0.05% w/v) (Sigma Aldrich, Poole, UK) containing EDTA (0.03% w/v) (Sigma Aldrich, Poole, UK) on achieving 70–90% confluency for seeding into 96 well test plates (cell density of 5 × 10^3 cells per well). The cells were allowed to adhere to the culture plates for 24 h before use.

For toxicity assessment, ricin toxin was diluted to 100 ng·mL^{-1} in culture medium and filtered using a 0.2 μm sterile filter before further dilution in culture medium and addition to the assay plate in triplicate. The plates were then incubated for 48 h prior to the addition of 10 μL of Roche Cell Proliferation Reagent WST-1 (Sigma Aldrich, Poole,UK). After 3 h the absorbance was read on a Thermo Multiskan plate reader (Thermo Fisher Scientific, Loughborough, UK) at 450 nm to assess cell viability.

5.4. In Vitro Neutralising Activity of Anti-Ricin Antitoxin

For in vitro neutralisation assays using the F(ab')$_2$ antitoxin, Vero cells were seeded into 96-well plates (5 × 10^3 per well) and incubated overnight 37 °C ± 5% CO_2. The F(ab')$_2$ antitoxin (73.4 ng·mL^{-1} to 3300 ng·mL^{-1}) was mixed with a fixed concentration of ricin (3.24 ng·mL^{-1}) for 1 h prior to the addition of the mixture to cells in the plate. A ricin cytotoxicity curve (3.56 ng·mL^{-1} to 0.001 ng·mL^{-1} ricin) was included on the plate in addition to media only (negative) controls. After 48 h incubation, 10 μL of WST-1 reagent (Sigma Aldrich, Poole, UK) was added and plates were incubated for a further 4 h at 37 °C at 5% CO_2. The absorbance was read at 450 nm.

Cytotoxicity data were normalised to the negative control values and analysed with a 4-parameter logistic fit (GraphPad Prism for Windows version 6.02). The neutralising ratio was determined from the calculated ricin LC_{50}, the antitoxin EC_{50} and the concentration of ricin used in the assay (3.24 ng·mL^{-1}) according to Equation (1).

$$\text{Neutralising ratio} = \frac{\text{Antitoxin } EC_{50}\left(\text{ng}\cdot\text{mL}^{-1}\right)}{3.24 - \text{Ricin } LC_{50}\left(\text{ng}\cdot\text{mL}^{-1}\right)}, \quad (1)$$

5.5. Animal Husbandry

All investigations involving animals conformed to the UK Animal (Scientific Procedures) Act 1986 and also the UK Codes of Practise for the Housing and Care of Animals Used in Scientific Procedures 1989 in an established process required to gain the UK Home Office Project Licence that covered this research (granted 30 October 2012). Age-matched female Balb/C mice (6–7 weeks old, Charles River Laboratories Ltd, Margate, Kent, UK) were used in all in vivo studies. On receipt, animals were acclimatised to the facility prior to being used on study. Mice were housed in rooms maintained at 21 °C ± 2 °C on a 12/12 h dawn to dusk cycle. Humidity was maintained at 55 ± 10% with airflow of 15–18 changes·h^{-1} and given water and food and water ad libitum. Mice were fed a standard pelleted Teklad TRM 19% protein irradiated diet (Harlan Teklad, Bicester, UK).

5.6. In Vivo Neutralisation Assay in Mice

Mice (10 per group) were randomly assigned to control or treatment groups and weighed on Day 0. The target weight range for animals on all studies was 17–21 g and no correction for body weight was made when dosing with ricin or antitoxin. Doses are therefore provided on a per mouse basis. On day zero, mice received one of a range of doses of ricin toxin between 0.22 and 0.77 μg per mouse (100 μL) via the i.p. route. The data were analysed with a probit model using Minitab (v17) to determine the LD_{50}. For in vivo neutralisation studies, a dose range of 56.2 to 93.6 μg antitoxin·mouse^{-1} F(ab')$_2$ was pre-incubated with 2 μg ricin·mouse^{-1} for 1 h and administered to Balb/C mice (10 per group) via the intraperitoneal route. Mice were observed at least twice daily for 14 days and the number of live and dead/moribund mice recorded at each observation. Moribund mice were culled upon reaching the humane end point (Table S1). Weight and visible signs of intoxication were also observed and recorded for 14 days. Dose–response data were analysed with a probit model using Minitab (v17) and the neutralizing ratio calculated from the antitoxin ED_{50}, the ricin LD_{50} value and the challenge dose of ricin (2 μg·mouse^{-1}) used according to Equation (2).

$$\text{Neutralising ratio} = \frac{\text{Antitoxin } ED_{50}\left(\text{ng}\cdot\text{mL}^{-1}\right)}{2 - \text{Ricin } LD_{50}\left(\text{ng}\cdot\text{mL}^{-1}\right)}, \quad (2)$$

5.7. Determination of Inhalational Toxicity of Ricin in Mice

Balb/C mice were exposed to aerosols of ricin (head only exposure) generated using a system previously described [5,30]. Each inhalation run had the capacity for the exposure of 12 mice. Animals were enclosed in whole body plethysmography tubes attached to the exposure line allowing individual respiratory parameters to be recorded. Mice (n = 12 per group) were exposed to targeted inhaled concentrations of ricin and survival and visible signs of intoxication (Table S1) were monitored for 14 days.

5.8. Efficacy of Ricin Antitoxins against Lethal Inhalation Ricin Challenge

Groups of mice (n = 8–12) received approximately a 3LCt_{50} aerosol challenge of ricin and 20 h following challenge, the indicated dose of ricin antitoxin was given by an intravenous (i.v.) injection. Mice were observed at least twice daily for 14 days and the number of live and dead/moribund mice recorded at each observation. Moribund mice were those that had reached the humane end point (severe piloerection, severe abdominal pinching and unable to move) and these mice were humanely killed. Weights and visible signs of intoxication were recorded daily for 14 days. Three independent

experiments were conducted (with up to 12 mice for each antitoxin dose group in each experiment). Control ricin-exposed mice received a vehicle (110 mM sodium chloride, 25 mM glycine and 1% v/v sucrose, pH 6.5–7.2) (all Sigma Aldrich, UK) injection. Mortality data were used to produce a dose–response relationship, which was analysed with a logistic model (GraphPad Prism for Windows version 6.02).

5.9. Intracellular Trafficking of Ricin and Fluorochome Labelled F(ab')$_2$

Ricin was labelled and experiments were conducted essentially as previously described (Jenner et al., 2017; manuscript submitted). F(ab')$_2$ was labelled using a microscale AF555 labelling kit (Thermo Life Sciences, Loughborough, UK). Briefly, F(ab')$_2$ was mixed with AF555 succinimidyl ester in a molar ratio of 13:1 in PBS buffer pH 8. The mix a incubated for 15 min at room temperature and the labelled F(ab')$_2$ purified from unbound dye using a NAP-5 column (GE Healthcare, Little Chalfont, UK). A549 cells were grown in Dulbecco's Modified Eagles Medium (DMEM; Gibco, ThermoFisher, Loughborough, UK) supplemented with 10% fetal bovine serum (Gibco,ThermoFisher, Loughborough, UK) and 2 mM glutamine (Gibco, ThermoFisher, Loughborough, UK) at 37 °C in a 5% CO_2 incubator with ~95% humidity. Cells were harvested with trypsin, enumerated and plated into a 24-well plate (Corning Costar) at a density of 5 × 10^5 cells·well^{-1}. Cells were incubated at 37 °C in a 5% CO_2 incubator with ~95% humidity for ~18 h to allow cell adherence to the plate. Media was removed from the wells and replaced with 200 µL of either a 1 µg·mL^{-1} ricin-AF647 solution or mixtures of the ricin with AF555-F(ab')$_2$, (equating to neutralising ratios of 1:20 (1 µg ricin, 20 µg F(ab')$_2$) or 1:50 (1 µg ricin, 50 µg F(ab')$_2$) for 1 h at 37 °C before being added to plated cells. The 1 µg·mL^{-1} concentration of ricin was used to enable visualisation of the fluorescence signal at the cellular level. This concentration of ricin is toxic to the cells (Figure 1), but is slightly less than concentrations used by others for confocal imaging of labelled ricin [51,52].

Exposed cells were then incubated for a range of times (15, 30 and 60 min) after which they were washed once with PBS before 200 µL detachin (AMS Biotechnology Limited, Abingdon, UK) was added. Cells were incubated at 37 °C for 3 min to allow detachment from the plate surface. Cells were then harvested and centrifuged at 300× *g* for 5 min and resuspended in 60 µL 4% paraformaldehyde. Cells were then counter stained with 1 µg Hoechst 33342 (ThermoFisher, Loughborough, UK) before data capture using Imaging Flow Cytometry.

5.10. Staining of Golgi Using Golgi-ID

Staining using Golgi-ID (Enzo Life Sciences, Exeter, UK) was achieved according to the manufacturer's instructions. Briefly, A549 cells were plated as previously described. Cells were incubated overnight and washed with 100 µL of assay solution before the addition of a 200 µL of Golgi-ID stain (1 in 100 dilution of provided stock solution) per well. Cells were then incubated at 4 °C for 30 min before removal of the Golgi-ID stain and washing of the cells with 100 µL assay buffer. A final 1 mL of DMEM was added to the cells and they were incubated for 30 min at 37 °C in a 5% CO_2 incubator with ~95% humidity before use in the ricin assays.

5.11. Imaging Flow Cytometry Data Collection and Analysis

IFC data were acquired using an ImageStream X MkII (ISX, Amnis, Seattle, WA, USA) equipped with dual cameras and 405, 488, 561 and 633 nm excitation lasers. All samples were acquired at ×60 magnification with a 0.9 NA objective, giving a 2.5 µm optical slice image and allowing colocalisation studies to be undertaken with this approach [65,66] A minimum of 7000 in-focus single cell events were collected for each sample. Only data from relevant channels were collected including Channel 01 (Ch01, brightfield camera 1), Channel 02 (Ch02, Golgi-ID, 488 nm laser power: 100 mW), Ch03 (AF555 F(ab')$_2$ 561 nm laser 200 mW), Channel 06 (Ch06, side scatter 785 nm laser power: 10 mW), Channel 07 (Ch07, Hoescht fluorescence 405 nm 120 mA laser power), Channel 09 (Ch09, brightfield camera 2) and Ch11 (AF647-ricin fluorescence 642 nm laser power: 150 mW). Data from samples with only single

stains were also captured to calculate the compensation matrix required to account for spectral overlap between the chosen fluorophores. All images shown are pseudo-coloured according to the following: nucleus = blue, Golgi = green, ricin = red, $F(ab')_2$ = yellow.

5.12. IFC Data Analysis

Analysis of IFC data was achieved using IDEAS® software (version 6.1). IDEAS® utilizes two main principles to make calculations from the images acquired these are masks and features. Masks are used to define regions of interest within the cell or fluorescence image. Those masks are used to calculate quantitative measurements from or within a masked region.

A mask was used to identify the cytoplasmic region of cells. The cytoplasmic mask was created by making an erode (M01, 8) mask (the default mask M01, eroded by 8 pixels around) and morphology (M07) mask of the nuclear channel. These two masks were then combined using Boolean logic (AND NOT) to make a mask that is specific for the cytoplasm. The full mask nomenclature for the cytoplasmic mask is: Erode (M01, 8) AND NOT Morphology (M07). When using Golgi-ID the default mask for the Golgi apparatus is not very specific, a more stringent mask was required to accurately reflect the Golgi location. To achieve this, a threshold mask is used; this masks a percentage of the brightest pixels within a given starting mask. Here, we have masked the top 70% of pixels within the default M02 mask. The nomenclature for this mask is Threshold (M02, Ch02, 70). All data shown is a percentage population using the in-focus single cells as the parent population. All modelling and statistical analysis was performed in GraphPad Prism version 6.02.

Supplementary Materials: The following are available online at www.mdpi.com/2072-6651/9/10/329/s1, Table S1: Scoring of observable signs of ricin intoxication in the mouse.

Acknowledgments: This research was funded by the UK Ministry of Defence. We wish to thank the animal services and veterinary staff at Dstl-Porton Down for enabling these studies to be conducted.

Author Contributions: G.D.G., S.J.C.W., D.C.J., G.C.C. and A.C.G. wrote the manuscript. R.J.G. provided the statistical analysis during the research. A.C.G. and J.L.H. reviewed the manuscript. All authors contributed to the research and/or data analysis.

Conflicts of Interest: The authors declare no conflict of interest.

References

1. Franz, D.R.; Jaax, N.K. Ricin toxin. In *Medical Aspects of Chemical and Biological Warfare*; Borden Institute, Walter Reed Army Medical Center: Washington, DC, USA, 1997; Chapter 32; pp. 631–642.
2. Shoham, D. Iraqs biological warfare agents: A comprehensive analysis. *Crit. Rev. Microbiol.* **2000**, *26*, 179–204. [CrossRef] [PubMed]
3. Roxas-Duncan, V.I.; Smith, L.A. Ricin: Perspective in bioterrorism. In *Bioterrorism*; Morse, S., Ed.; InTech: Rijeka, Croatia, 2012; Volume 7, pp. 133–158.
4. Worbs, S.; Köhler, K.; Pauly, D.; Avondet, M.-A.; Schaer, M.; Dorner, M.B.; Dorner, B.G. *Ricinus communis* intoxications in human and veterinary medicine-a summary of real cases. *Toxins* **2011**, *3*, 1332–1372. [CrossRef] [PubMed]
5. Griffiths, G.D.; Phillips, G.J.; Holley, J.L. Inhalation toxicology of ricin preparations: Animal models, prophylactic and therapeutic approaches to protection. *Inhal. Toxicol.* **2007**, *19*, 873–887. [CrossRef] [PubMed]
6. Lord, J.M.; Griffiths, G.D. Ricin: Chemistry, sources, exposures, toxicology and medical aspects. In *General, Applied and Systems Toxicology*; Wiley Ltd.: Chichester, UK, 2009. [CrossRef]
7. Reisler, R.B.; Smith, L.A. The need for continued development of ricin countermeasures. *Adv. Prev. Med.* **2012**, *1*, 1–4. [CrossRef] [PubMed]
8. Barbieri, L.; Baltelli, M.; Stirpe, F. Ribosomes-inactivating proteins from plants. *Biochem. Biophys. Acta* **1993**, *1154*, 237–282. [CrossRef]
9. Lord, J.M.; Roberts, L.M.; Robertus, J.D. Ricin: Structure, mode of action and some current application. *FASEB J.* **1994**, *8*, 201–208. [CrossRef] [PubMed]

10. Rutenber, E.; Robertus, J.D. Structure of ricin B-chain at 2.5 A resolution. *Proteins Struct. Funct. Genet.* **1991**, *10*, 260–269. [CrossRef] [PubMed]
11. Khan, T.; Waring, P. Macrophage adherence prevents apoptosis induced by ricin. *Eur. J. Cell Biol.* **1993**, *62*, 406–414. [PubMed]
12. Simmons, B.M.; Stahl, P.D.; Russell, J.H. Mannose receptor mediated uptake of ricin toxin and ricin A-chain by macrophages. Multiple intracellular airways for A chain translocation. *J. Biol. Chem.* **1986**, *261*, 7912–7920. [PubMed]
13. Magnusson, S.; Berg, T. Endocytosis of ricin by rat liver cells in vivo and in vitro is mainly mediated by mannose receptors on sinusoidal endothelial cells. *Biochem. J.* **1994**, *291*, 749–755. [CrossRef]
14. Sapoznikov, A.; Falach, R.; Mazor, O.; Alcalay, R.; Gal, Y.; Seliger, N.; Sabo, T.; Kronman, C. Diverse profiles of ricin-cell interactions in the lung following intranasal exposure to ricin. *Toxins* **2015**, *7*, 4817–4831. [CrossRef] [PubMed]
15. Lord, J.M.; Smith, D.C.; Roberts, L.M. Toxin entry: How bacterial proteins get into mammalian cells. *Cell Microbiol.* **1991**, *1*, 85–91. [CrossRef]
16. Robertus, J. The structure and action of ricin: A cytotoxic N-glycosidase. *Cell Biol.* **1991**, *2*, 23–30.
17. Eiklid, K.; Olsnes, S.; Pihl, A. Entry of lethal doses of abrin, ricin and modeccin into the Cytosol of HeLa cells. *Exp. Cell Res.* **1980**, *126*, 321–326. [CrossRef]
18. Olsnes, S.; Kozlov, J.V. Ricin. *Toxicon* **2001**, *39*, 1723–1728. [CrossRef]
19. Soler-Rodriguez, A.-M.; Ghetie, M.-A.; Oppenheimer-Marks, N.; Uh, J.W.; Vitetta, E.S. Ricin A-chain and ricin A-chain immunotoxins rapidly damage human endothelial cells, Implications for vascular leak syndrome. *Exp. Cell Res.* **1993**, *206*, 227–234. [CrossRef] [PubMed]
20. Lindauer, M.L.; Wong, J.; Iwakura, Y.; Magun, B.E. Pulmonary inflammation triggered by ricin toxin requires macrophages and IL-1 signalling. *J. Immunol.* **2009**, *183*, 1419–1426. [CrossRef] [PubMed]
21. Mabley, J.G.; Pacher, P.; Szabo, C. Activation of cholinergic anti-inflammatory pathway reduces ricin-induced mortality and organ failure in mice. *Mol. Med.* **2009**, *15*, 166–172. [CrossRef] [PubMed]
22. Gal, Y.; Mazor, O.; Alcalay, R.; Seliger, N.; Aftalion, M.; Sapoznikov, A.; Falach, R.; Kronman, C.; Sabo, T. Antibody/doxycycline combined therapy for pulmonary ricinosis: Attenuation of inflammation improves survival of ricin-intoxicated mice. *Toxicol. Rep.* **2014**, *1*, 496–504. [CrossRef] [PubMed]
23. Sabo, T.; Gal, Y.; Elhanany, E.; Sapoznikov, A.; Falach, R.; Mazor, O.; Kronman, C. Antibody treatment against pulmonary exposure to abrin confers significantly higher levels of protection than treatment against ricin intoxication. *Toxicol. Lett.* **2015**, *237*, 72–78. [CrossRef] [PubMed]
24. Roy, C.J.; Song, K.; Sivasubramani, S.K.; Gardner, D.J.; Pincus, S.H. Animal models of ricin toxicosis. *Curr. Top. Microbiol. Immunol.* **2012**, *357*, 243–257. [PubMed]
25. Godal, A.; Fodstad, O.; Ingebrigtsen, K.; Pihl, A. Pharmacological studies of ricin in mice and humans. *Cancer Chemother. Pharmacol.* **1984**, *13*, 157–163. [CrossRef] [PubMed]
26. Fodstad, O.; Olsnes, S.; Pihl, A. Toxicity, distribution and elimination of the cancerostatic lectins abrin and ricin after parenteral injections into mice. *Br. J. Cancer* **1976**, *32*, 418–425. [CrossRef]
27. Griffiths, G.D.; Leek, M.D.; Gee, D.J. The toxic plant proteins ricin and abrin induce apoptotic changes in mammalian lymphoid tissues and intestines. *J. Pathol.* **1987**, *151*, 221–229. [CrossRef] [PubMed]
28. Balint, G.A. Ricin: The toxic protein of castor oil seeds. *Toxicology* **1974**, *2*, 77–102. [CrossRef]
29. Muldoon, D.F.; Stoh, S.J. Modulation of ricin toxicity in mice by biologically active substances. *J. Appl. Toxicol.* **1994**, *14*, 81–86. [CrossRef] [PubMed]
30. Griffiths, G.D.; Rice, P.; Allenby, A.C.; Bailey, S.C.; Upshall, D.G. Inhalation toxicology and histopathology of ricin and abrin toxins. *Inhal. Toxicol.* **1995**, *7*, 269–288. [CrossRef]
31. Bhaskaran, M.; Didier, P.J.; Sivasubramani, S.K.; Doyle, L.A.; Holley, J.; Roy, C.J. Pathology of lethal and sublethal doses of aerosolized ricin in Rhesus Macaques. *Toxicol. Pathol.* **2014**, *42*, 573–581. [CrossRef] [PubMed]
32. Mayers, C.N.; Holley, J.L.; Brooks, T. Antitoxin therapy for botulinum intoxication. *Rev. Med. Microbiol.* **2001**, *12*, 1–9. [CrossRef]
33. Casadevall, A. Passive antibody administration as a specific defence against biological weapons. *Emerg. Infect. Dis.* **2002**, *8*, 833–841. [CrossRef] [PubMed]
34. Chippaux, J.P.; Goyffon, M. Venoms, anti-venoms and immunotherapy. *Toxicon* **1998**, *36*, 823–846. [CrossRef]

35. Sedlacek, H.H.; Gronski, P.; Hofstaetter, E.J.; Kanzy, E.J.; Schlorlemmer, H.U.; Seiler, F.R. The biological properties of Immunoglobulin G and its split products (Fab')2 and Fab. *Klin. Wochenschr.* **1983**, *61*, 723–736. [CrossRef] [PubMed]
36. Nydegger, U.E.; Sturzenegger, M. Adverse effects of intravenous immunoglobulinum therapy. *Drug Saf.* **1999**, *21*, 171–185. [CrossRef] [PubMed]
37. Morais, V.M.; Massaldi, H. Snake antivenoms: Adverse reactions and production technology. *Venom. Anim. Toxins Incl. Trop. Dis.* **2009**, *15*, 2–18. [CrossRef]
38. O'Hara, J.M.; Whaley, K.; Pauly, M.; Zeitlin, L.C.; Mantis, N. Plant-based expression of a partially humanized neutralizing monoclonal IgG directed against an immunodominant epitope on the ricin toxin A subunit. *Vaccine* **2012**, *30*, 1239–1243. [CrossRef] [PubMed]
39. Sully, E.K.; Whaley, K.J.; Bohorova, N.; Goodman, C.; Kim, D.H.; Pauly, M.H.; Velasco, J.; Hiatt, E.; Morton, J.; Swope, K.; et al. Chimeric plantibody passively protects mice against aerosolized ricin challenge. *Clin. Vaccine Immunol.* **2014**, *21*, 777–782. [CrossRef] [PubMed]
40. Van Slyke, G.; Sully, E.K.; Bohorova, N.; Bohorov, O.; Kim, D.; Pauly, M.; Whaley, K.; Zeitlin, L.; Mantis, N.J. A humanized monoclonal antibody that passively protects mice 3 against systemic and intranasal ricin toxin challenge. *Clin. Vaccine Immunol.* **2016**. [CrossRef] [PubMed]
41. Pratt, T.S.; Pincus, S.H.; Hale, M.L.; Moreira, A.L.; Roy, C.J.; Tchou-Wong, K.-M. Oropharyngeal aspiration of ricin as a lung challenge model for evaluation of the therapeutic index of antibodies against ricin A chain for post-exposure treatment. *Exp. Lung Res.* **2007**, *33*, 459–481. [CrossRef] [PubMed]
42. Noy-Porat, T.; Alcalay, R.; Epstein, E.; Sabo, T.; Kronman, C. Extended therapeutic window for post exposure treatment of ricin intoxication conferred by the use of high-affinity antibodies. *Toxicon* **2017**, *127*, 100–105. [CrossRef] [PubMed]
43. Miner, N.A.; Koehler, J. Intraperitoneal injection of mice. *Appl. Microbiol.* **1968**, *16*, 1418–1419.
44. Noy-Porat, T.; Rosenfeld, R.; Ariel, N.; Epstein, E.; Alcalay, R.; Zvi, A.; Kronman, C.; Ordentlich, A.; Mazor, O. Isolation of anti-ricin protective antibodies exhibiting high affinity from immunized non-human primates. *Toxins* **2016**, *8*, 64. [CrossRef] [PubMed]
45. Griffiths, G.D.; Lindsay, C.D.; Upshall, D.G. Examination of the toxicity of several protein toxins of plant origin using bovine pulmonary endothelial cells. *Toxicology* **1994**, *90*, 11–27. [CrossRef]
46. Yermakova, A.; Mantis, N.J. Protective immunity to ricin toxin conferred by antibodies against the toxin's binding subunit (RTB). *Vaccine* **2011**, *29*, 7925–7935. [CrossRef] [PubMed]
47. Wei, G.; Hu, W.-G.; Yin, J.; Chau, D.; Hu, C.C.; Lillico, D.; Yu, J.; Negrych, L.M.; Cherwonogrodzky, J.W. Conformation-dependent high-affinity potent ricin-neutralizing monoclonal antibodies. *Biomed. Res. Int.* **2013**. [CrossRef]
48. Hu, W.G.; Yin, J.; Chau, D.; Negreych, L.M.; Cherwonogrodzky, J.W. Humanization and characterization of an anti-ricin neutralization monoclonal antibody. *PLoS ONE* **2012**, *7*, e45595. [CrossRef] [PubMed]
49. Prigent, J.; Panigai, L.; Lamourette, P.; Sauvaire, D.; Devilliers, K.; Plaisance, M.; Volland, H.; Creminon, C.; Simon, S. Neutralising antibodies against ricin toxin. *PLoS ONE* **2009**, *6*, e20166. [CrossRef] [PubMed]
50. Herrera, C.; Klokk, T.; Cole, R.; Sandvig, K.; Mantis, N.J. A bispecific antibody promotes aggregation of ricin toxin on cell surfaces and alters dynamics of toxin internalization and trafficking. *PLoS ONE* **2016**, *11*, e0156893. [CrossRef] [PubMed]
51. Song, K.; Mize, R.R.; Marrero, L.; Corti, M.; Kirk, J.M.; Pincus, S.H. Antibody to ricin A chain hinders intracellular routing of toxin and protects cells even after toxin has been internalized. *PLoS ONE* **2013**, *8*, e62417. [CrossRef] [PubMed]
52. Yermakova, A.; Klokk, T.I.; Cole, R.; Sandvig, K.; Mantis, N.J. Antibody-mediated inhibition of ricin toxin retrograde transport. *mBio* **2014**, *5*, e00995. [CrossRef] [PubMed]
53. Yermakova, A.; Klokk, T.I.; O'Hara, J.M.; Cole, R.; Sandvig, K.; Mantis, N.J. Neutralizing monoclonal antibodies against disparate epitopes on ricin toxin's enzymatic subunit interfere with intracellular toxin transport. *Sci. Rep.* **2016**, *6*, 22721. [CrossRef] [PubMed]
54. Gawarammana, I.; Keyler, D. Dealing with adverse reactions to snake venom. *Ceylon Med. J.* **2011**, *56*, 87–90. [CrossRef] [PubMed]
55. Theakston, R.D.G.; Smith, D.C. Therapeutic antibodies to snake venoms. In *Therapeutic Antibodies*; Landon, J., Chard, T., Eds.; Springer: London, UK, 1995; Chapter 6, pp. 109–133.

56. Mayers, C.N.; Veall, S.; Bedford, R.J.; Holley, J.L. Anti-immunoglobulin responses to IgG, F(ab')2 and Fab botulinum antitoxins in mice. *Immunopharmacol. Immunotoxicol.* **2003**, *25*, 397–408. [CrossRef] [PubMed]
57. Holley, J.L.; Poole, S.J.C.; Cooper, I.A.M.; Griffiths, G.D.; Simpson, A.J. The production and evaluation of ricin antitoxin. In *Defence against the Effects of Chemical Hazards: Toxicology, Diagnosis and Medical Countermeasures*; NATO Meeting Proceedings RTO-MP-HFM-149; NATO: Neuilly-sur-Seine, France, 2007; pp. 12-1–12-8.
58. Sesardic, D.; Winsnes, R.; Rigsby, P.; Beh-Gross, M.-E. Collaborative study for the calibration of serological methods for potency testing of diphtheria toxoid vaccines. Extended study: Correlation of serology with in vivo toxin neutralisation. *Pharmeuropa Bio* **2003**, *2*, 69–75.
59. *First WHO International Standard for Human Diphtheria Antitoxin*; WHO Expert Committee on Biological Standardization: 63rd Report; World Health Organization: Geneva, Switzerland, 2013; Section 4.1.3, p. 29.
60. Stechmann, B.; Bai, S.K.; Gobbo, E.; Lopez, R.; Merer, G.; Pinchard, S.; Panigai, L.; Tenza, D.; Raposo, G.; Beaumelle, B.; et al. Inhibition of retrograde transport protects mice from lethal ricin challenge. *Cell* **2010**, *141*, 231–242. [CrossRef] [PubMed]
61. Barbier, J.; Bouclier, C.; Johannes, L.; Gillet, D. Inhibitors of the cellular trafficking of ricin. *Toxins* **2012**, *4*, 15–27. [CrossRef] [PubMed]
62. Gupta, N.; Pons, V.; Noel, R.; Buisson, D.A.; Uisson, D.A.; Michau, A.; Johannes, L.; Gillet, D.; Barbier, J.; Cintrat, J.-C. (S)-N-Methyldihydroquinazolinones are the Active Enantiomers of Retro-2 Derived Compounds against toxins. *ACS Med. Chem. Lett.* **2014**, *5*, 94–97. [CrossRef] [PubMed]
63. Gal, Y.; Sapoznikov, A.; Falach, R.; Ehrlich, S.; Aftalion, M.; Sabo, T.; Kronman, C. Potent antiedematous and protective effects of ciprofloxacin in pulmonary ricinosis. *Antimicrob. Agents Chemother.* **2016**, *60*, 7153–7158. [PubMed]
64. Thullier, P.; Griffiths, G.D. Broad recognition of ricin toxins prepared from a range of *Ricinus* cultivars using immunochomatographic tests. *Clin. Toxicol.* **2009**, *47*, 643–650. [CrossRef] [PubMed]
65. Pugsley, H.R. Quantifying autophagy: Measuring LC3 puncta and autolysosome formation in cells using multispectral imaging flow cytometry. *Methods* **2017**, *112*, 147–156. [CrossRef] [PubMed]
66. Rajan, R.; Karbowniczek, M.; Pugsley, H.R.; Sabnani, M.K.; Astrinidis, A.; La-Beck, N.M. Quantifying autophagosomes and autolysosomes in cells using imaging flow cytometry. *Cytometry A* **2015**, *87*, 451–458. [CrossRef] [PubMed]